Journal of Photochemistry and Photobiology 3–4 (2020) 100011

Contents lists available at ScienceDirect

Journal of Photochemistry and Photobiology

journal homepage: www.elsevier.com/locate/jpap

Fluorine induced conformational switching and modulation in photophysical properties of 7-fluorotryptophan: Spectroscopic, quantum chemical calculation and molecular dynamics simulation studies

Tonima Nandy, Saptarsi Mondal, Prashant Chandra Singh*

School of Chemical Sciences, Indian Association for the Cultivation of Science, 2A &2B Raja S. C. Mullick Road, Jadavpur, Kolkata 700032, India

ARTICLE INFO

Keywords:
Fluorotryptophan
Photophysical properties
Quantum chemical calculation
Molecular dynamics simulation

ABSTRACT

7-Fluorotryptophan (7F-Trp) is an important noncanonical derivative of tryptophan (Trp) amino acid which depicts high in vivo stability for the positron emission tomography imaging of Trp metabolism. Irrespective of biological importance of 7F-Trp, molecular level understanding about its fluorescence behavior and the photophysical properties in different solvents are still unknown. Hence, the photophysical properties of 7F-Trp in presence of biochemically important alcoholic solvents ethanol (ETH), 2,2,2 trifluoroethanol (TFE) and 1,1,1,3,3,3-hexafluoro-propan-2-ol (HFIP) has been investigated using spectroscopic, quantum chemical calculation, molecular dynamic simulation and compared with Trp to understand the role of fluorine in its fluorescence behavior. The substitution of fluorine on Trp decreases its fluorescence intensity significantly. The presence of fluorine on tryptophan perturbs the interaction of its backbone containing COO^- and NH_3^+ with the chromophoric indole group which probably decreases the barrier of the conical intersection leading to decreased fluorescence intensity of 7F-Trp compared to Trp. The fluorescence intensity of Trp and 7F-Trp decreases in presence of fluorinated alcohols compared to ETH. However, the decrease in fluorescence intensity of 7F-Trp is less than Trp and peak maxima are blue shifted. Moreover, the trend of excited state lifetime of 7F-Trp in fluorinated alcohols is opposite to Trp suggesting that the interaction of 7F-Trp with fluorinated solvents is different than Trp. The excited state lifetime of Trp in alcoholic solvents is controlled mainly by solvent polarity. In contrast, the weak interaction mediated by the fluorine of 7F-Trp with the fluorine and OH groups of fluorinated solvents plays an important role in modulation of its excited state lifetime. This study clearly depicts that noncanonical fluorine of 7F-Trp plays an important role in controlling its fluorescence properties in the biochemically important alcoholic solvents.

Introduction

Biosynthesis of protein is controlled by twenty amino acids which affect several functionality of an organism. Tryptophan (Trp) is one of the important aromatic amino acids whose intrinsic fluorescence property has been utilized to characterize the structure of proteins in different environments [1]. Extensive studies have been performed to characterize the fluorescence properties of Trp which gets markedly affected by solvent environment, conformational change of protein, and different quenching processes [2-6]. The functional limitation of proteins due to the limited number of natural amino acids prompts the development of new modified amino acids known as noncanonical amino acids which enhances the understanding about the complex functionality and novel chemistry of proteins. In this line, several modified Trp have been synthesized to understand the different complex processes associated with proteins such as folding, solvation, aggregation, interaction with other biomolecules like DNA, RNA, etc. [7-9].

Fluorinated amino acids are one of the important noncanonical amino acids which have been extensively used to understand the protein-protein, membrane-protein interactions, modification of the protein's functionality and enhancement of the stability of protein and enzymes without much affecting their structures [10-15]. Indeed, It has been shown that the incorporation of fluorinated Trp enhances catabolic activity by several folds as compared to Trp [16]. Although fluorocarbon and hydrocarbon both are hydrophobic in nature; polarizability of fluorocarbon group is less than hydrocarbon group due to its high electronegativity and small charge. The dipole moment of C-F is higher and is of opposite direction than C-H group. Indeed, the higher dipole

* Corresponding author.
E-mail address: sppcs@iacs.res.in (P.C. Singh).

https://doi.org/10.1016/j.jpap.2020.100011
Received 9 July 2020; Received in revised form 13 October 2020; Accepted 13 November 2020
Available online 20 November 2020
2666-4690/© 2020 The Authors. Published by Elsevier B.V. This is an open access article under the CC BY-NC-ND license (http://creativecommons.org/licenses/by-nc-nd/4.0/)

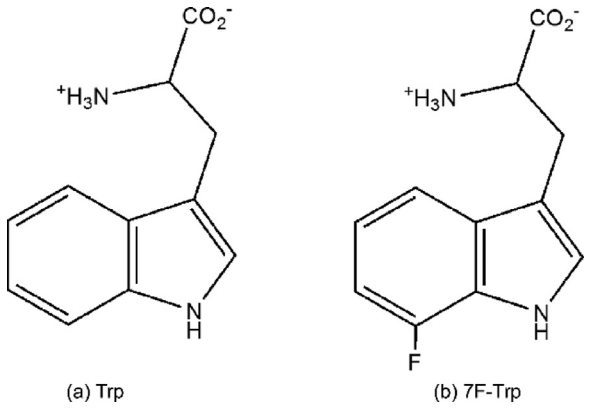

Fig. 1. The molecular (zwitterionic) structure of Trp and 7F-Trp are shown in (a) and (b), respectively.

moment of C-F group exerts electrostatic interaction on the neighboring solvent molecules, hence, the hydrophobicity of the C-F group is known as polar hydrophobicity [17].

The effect of the incorporation of fluorinated amino acids on the hydration of protein was studied by Zewail and coworkers and found that the side chain fluorination of protein exerts strong electrostatic drag on water molecules which slows down reorientation of water near the fluorinated surface [18]. Kunston and coworkers incorporated 5-fluoroTrp in monellin which provides the distinct ultrafast relaxation purely due to solvent and protein response [19]. Krishnamoorthy and coworkers have shown that the incorporation of 5-fluoroTrp in proteins decreases the lifetime heterogeneity as compared to tryptophan [20]. Recent study of the different fluorinated tryptophan derivatives in the cellular uptake study suggests that 7-fluorotryptophan (7F-Trp) depict high in vivo stability and enable a clear delineation of serotonergic areas and melatonin pineal gland in rat brains compared to 4, 5 and 6 fluoro substituted tryptophan [21]. Trp metabolism has been implicated in the various pathways like neuropathogenesis of HIV, serotonin, melatonin and NAD^+ etc. [22]. Moreover, tryptophan metabolism has been used as a new target for the treatment of schizophrenia, a mental illness [23]. 7F-Trp has been suggested as a potential candidate for the positron emission tomography imaging of Trp metabolism [21]. The fluorescence of 7F-Trp can be used as a reporter of local environment of Trp for which complete knowledge of its photophysical properties is very important. Irrespective of the importance of 7F-Trp in several biological activities, the molecular level understanding about its photophysical as well as fluorescence properties in different solvents is elusive.

In order to probe the role of the solvent organization and its interaction with the noncanonical part of Trp in its fluorescence properties, we have investigated the photophysical properties of Trp and 7F-Trp (chemical structures are shown in Fig. 1) in the presence of biochemically important alcoholic solvents namely, ethanol (ETH), 2,2,2-trifluoroethanol (TFE) and 1,1,1,3,3,3-hexafluoro-propan-2-ol (HFIP), respectively using spectroscopic, quantum chemical calculation and molecular dynamic (MD) simulation. Fluorinated-ETHs have been chosen as it is well known that they act as cosolvents to stabilize the secondary structure of proteins as well as induce the change in their conformation [24,25]. The hydrophobic CF_3 group of TFE favorably surrounds the protein leading to dehydration of protein backbone which promotes stabilization of the secondary structure of protein. TFE is also used in biochemistry as an inhibitor of alcohol dehydrogenase [26]. Similarly, HFIP has been used as a primary metabolite of the anesthetic sevoflurane which is known to provide beneficial immunomodulatory effects and the same effect can be obtained by intravenous administration of HFIP due to the presence of fluorocarbon groups [27,28]. A recent work claims that the effect of administration of HFIP intravenously in attenuating inflammation has been found to be equal or sometimes superior compared to inhaled sevoflurane [29]. HFIP may also provide the important structural insights of some unknown drugs and proteins [30,31]. This study suggests that the conformation of 7F-Trp is different in the ground and excited state as compared to Trp which causes to the decrease in its fluorescence. It has been found that the excited state lifetime trend of 7F-Trp is opposite to Trp in fluorinated alcohols due to the weak interaction of fluorine of 7F-Trp with the fluorine as well as OH terminals of fluorinated alcohols.

Materials and methods

Trp (99%) and 7F-Trp (99%) were purchased from SRL Pvt. Ltd. and Sigma-Aldrich, respectively. ETH (99.9%), TFE (99%) and HFIP (99.5%) were purchased from Spectrochem Pvt. Ltd., Mumbai, India. All the chemicals were used as received.

The UV–visible and fluorescence spectra of samples were measured using Evolution 201 (Thermo Fisher Scientific) and Fluoromax 4 (HORIBA JobinYvon Scientific) spectrometers, respectively. The fluorescence intensity decays of the samples were measured using the time-correlated single-photon counting (TCSPC) setup of Deltaflex (HORIBA). The excitation source of 280 nm was used for the TCSPC measurements. The FWHM of the excitation source was found to be ~ 900 ps which were measured using liquid scatterer. The emission was collected at the magic angle polarization and detected using a multiple channel photomultiplier (HPPD-C1). The decay traces were fit using the EzTime software. The reliability of the fitting was checked by using the reduced chi-square (χ^2) and distribution of the residual methods. The χ^2 value of the fitting was found to be close to one and the distribution of the residual was uniformly distributed around zero line. The concentration of the sample was kept ~50 μM for these measurements and all the experiments were performed at room temperature. Quantum yield of Trp and 7F-Trp in all the solvents were calculated using the standard protocol and details of the calculation have been provided in the supporting information.

Several different conformers of Trp and 7F-Trp were created using the semiempirical method which was further optimized using the M06-2X/ 6-31+g(d) level of theory [32] (Figure S1) to get the minimum energy structure of these molecules. All the optimization has been performed in solvent medium which has been implemented using the polarizable continuum model (PCM) [33]. It is important to mention that the PCM model has certain limitations in including the complete effect of solvent as it only includes the electrostatic interaction and excludes the effect of weak dispersive interaction [34]. The optimization of each structure has been performed in the ground as well as excited states. Frequency calculation of each structure depicts positive value which confirms that the optimized structure is stable in nature. Further, different structures of 1:1 cluster of Trp and 7F-Trp with ETH and TFE in their respective bulk medium were optimized in the ground as well as excited states to understand the mode of the binding of Trp and 7F-Trp with solvent molecules. The emission maxima of monomer of Trp and 7F-Trp and its clusters with solvent molecules were calculated to understand its fluorescence properties in different solvents. To rationalize the spectral shift qualitatively, HOMO–LUMO energy calculation has also been performed for both amino acids using the same level of theory. All the quantum chemical calculations were performed using the Gaussian 16 suites of program [35]. In order to characterize the interaction between the solvent and amino acids, we have performed the Atoms in molecule (AIM) calculation using AIM 2000 software [36].

Molecular dynamics (MD) simulation of Trp and 7F-Trp in ETH and TFE solvents were performed using GROMACS molecular dynamics simulation package (version 5.1) [37] to understand the solvent orientation around the different groups of amino acids and its correlation with fluorescence properties. Optimized potential for liquid simulation for all atom (OPLS-AA) force field [38] was used for the simulation of these systems. The OPLS-AA force field for TFE, Trp and 7F-Trp was generated using the LigPargen software [39-41] whereas, default OPLS-AA

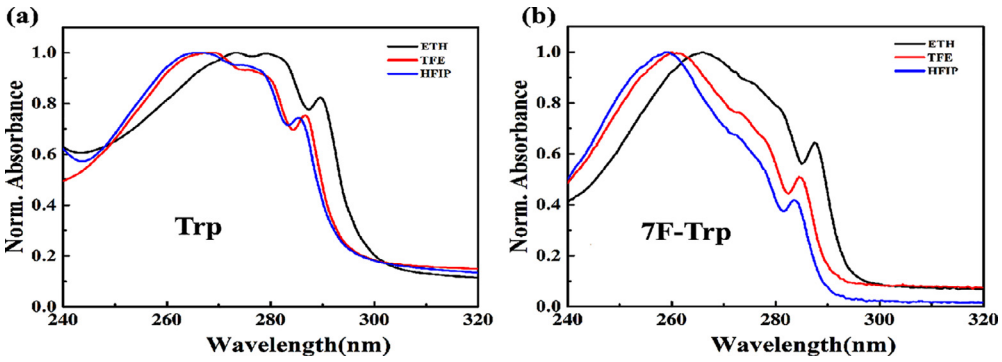

Fig. 2. The normalized absorption spectra of (a) Trp and (b) 7F-Trp in ETH, TFE and HFIP, respectively.

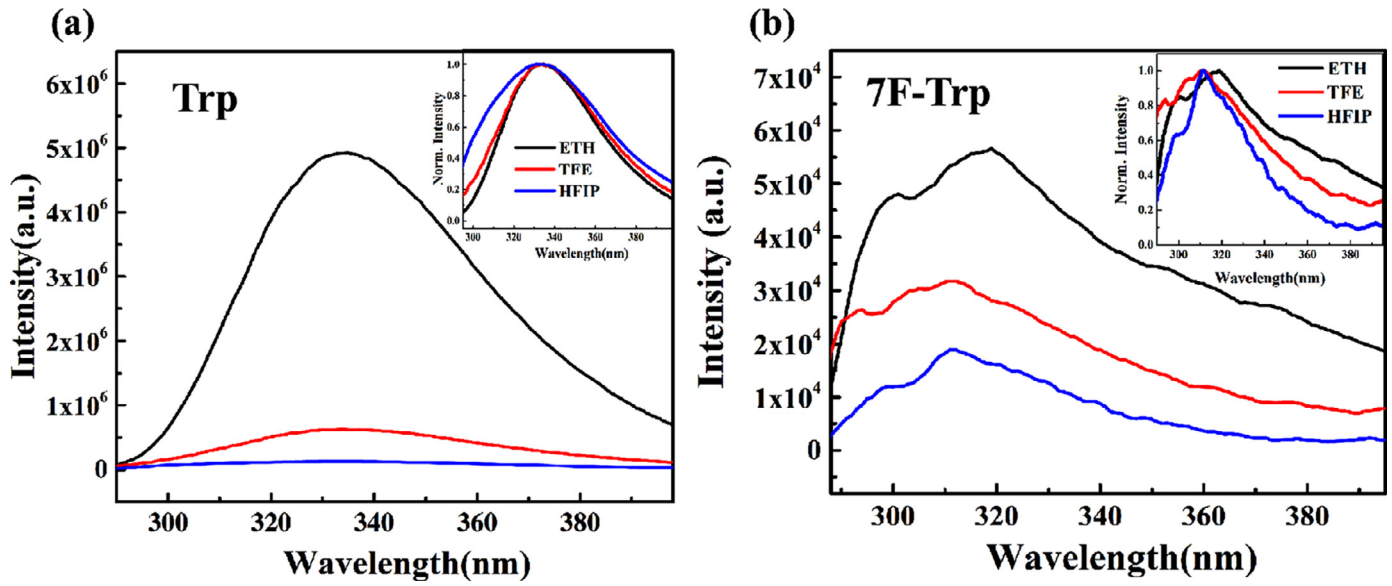

Fig. 3. The steady state emission spectra of (a) Trp and (b) 7F-Trp in ETH, TFE and HFIP, respectively. The normalized emission spectra are shown in inset.

force field available in Gromacs topology was used for ETH. Each amino acid was solvated with ~ 4000 solvents molecules to generate bulk like environment. In order to remove the unfavorable interaction from the initial structure of the system, energy minimization using the 1000 steps of steepest descent method was performed. Further, each trajectory was equilibrated in NPT ensemble for 1 ns at 298 K temperature and 1 bar pressure. Finally, the production run of 50 ns along with the periodic boundary condition in the NPT ensemble at 298 K temperature and 1 bar pressure was performed. The pressure and temperature of the system was kept constant by using the Parrinello–Rahman barostat [42] with time constant of 1.0 ps and Berendsen thermostat [43] of 0.1 ps time constant. Electrostatic interactions were incorporated using the Particle Mesh Ewald (PME) [44] with a grid spacing of 0.16 nm. Non-bonded force calculation with a grid was used for the generation of neighbor list which was updated after every 5 second. In order to understand the fluorescence properties, the MD simulation of Trp and 7F-Trp in ETH and TFE solvents were performed using their excited state charge distribution which has been obtained by the quantum chemical calculation. The radial distribution function g(r) calculation for the different sites of amino acids with solvent molecules was performed to get the role of interaction of solvent molecules in its fluorescence properties. To model the interactions involving halogen atoms, a new concept of sigma-hole has drawn significant interest but it is important to note that this effect is more effective for heavy atom like iodide and gradually decreasing like bromide> chloride>fluoride [45-48]. However, for fluoro-compound the effect is almost negligible; hence, we have used classical force field without considering sigma-hole concept.

Results and discussion

The absorption spectra of Trp and 7F-Trp in ETH, TFE and HFIP are shown in Fig. 2. The absorption features of Trp and 7F-Trp are structured in all the solvents suggesting that both L_a and L_b states [49] contribute to their absorption spectrum. Noticeably, the band position and the band shape of the absorption spectra of Trp are different from 7F-Trp in all the alcoholic solvents. The absorption spectra get blue shifted on the fluorination of Trp as well as the intensity ratio of the peak centered around 270 and 260 nm get changed which suggests that the fluorination of Trp changes the contribution of the mixing of L_a and L_b states in their absorption spectra. Nevertheless, the absorption spectra of Trp and 7F-Trp show the same trend in alcoholic solvents and get blue shifted with the fluorination of alcohol.

In order to understand the photophysical properties of noncanonical amino acid in alcoholic solvents, we have measured the emission spectra of Trp and its fluorinated analogue in the same solvents using excitation wavelength 280 nm as shown in Fig. 3. It can be seen that the fluorescence intensity of 7F-Trp is significantly less than Trp in any alcoholic solvents which suggests that the substitution of fluorine quenches the fluorescence intensity of Trp. Apart from the intensity change, the emission spectra get blue shifted with the fluorination of Trp as the fluorescence maxima of Trp and 7F-Trp appears at 335 and 310 nm, respectively. The data obtained from the emission spectra suggest that fluorination of Trp destabilizes the excited state as well as increases the rate of nonradiative process. The fluorescence intensity of both, Trp and 7F-Trp decreases with the fluorination of alcoholic

Table 1
The steady state emission maxima (λ_{max}), excited state lifetime (τ) along with their relative amplitude (a), average life time ($<\tau>$), quantum yield (ϕ), radiative rate constant (K_r) and non-radiative rate constant (K_{nr}) as well as χ^2 value of each fitted curve.

System	Emission (λ_{max}) (nm)	τ_1 (ns)	a_1	τ_2 (ns)	a_2	χ^2	$<\tau>$	ϕ	$K_r \times 10^{-6}$ (s^{-1})	$K_{nr} \times 10^{-8}$ (s^{-1})
Trp										
ETH	335	1.80±0.05	0.76	4.90±0.20	0.24	0.96	2.10±0.20	0.219	104.3	3.7
TFE	335	0.39±0.02	0.91	1.94±0.20	0.09	1.03	0.42±0.10	0.016	38.1	23.4
HFIP	335	0.21±0.03	0.82	3.45±0.20	0.18	1.04	0.25±0.10	0.002	8.0	39.9
7F-Trp										
ETH	320	0.80±0.02	0.61	4.50±0.10	0.39	1.14	1.16±0.10	0.003	2.6	8.6
TFE	310	0.82±0.02	0.54	4.90±0.10	0.46	1.11	1.33±0.10	0.001	0.7	7.5
HFIP	310	0.98±0.03	0.48	4.44±0.08	0.52	1.11	1.64±0.09	0.001	0.6	6.1

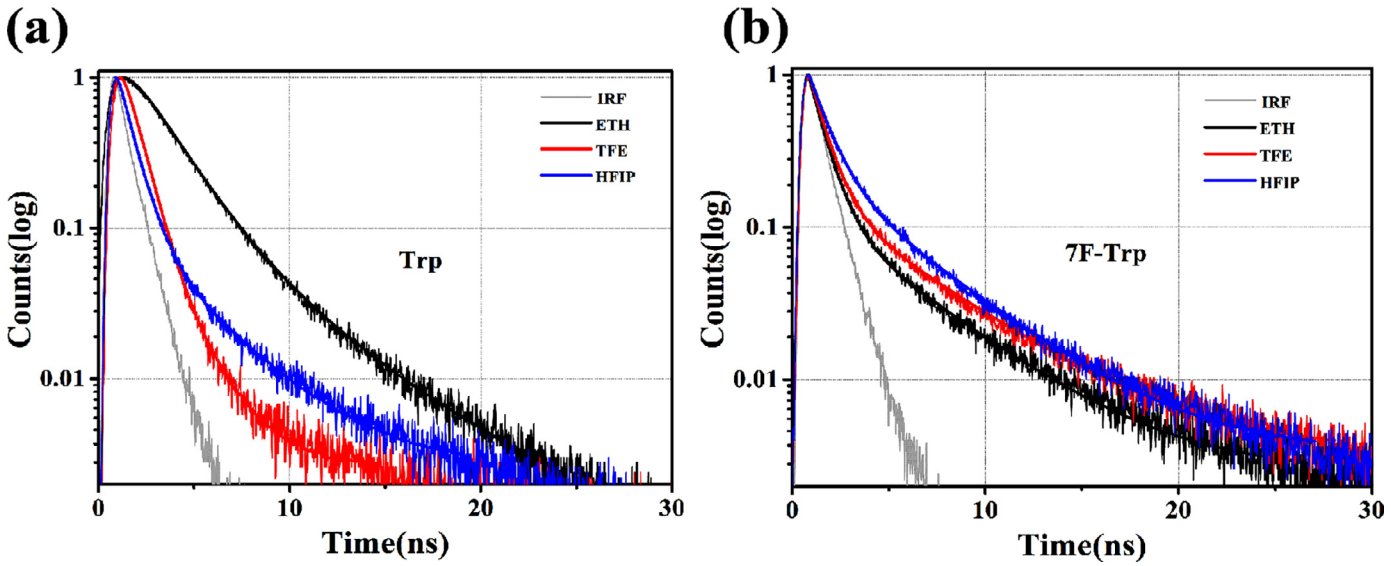

Fig. 4. The excited state fluorescence decay of (a) Trp and (b) 7F-Trp at their respective emission maxima along with their fitting lines in ETH, TFE and HFIP solvents respectively. The instrumental response function has been shown in ash line.

solvents indicating that the increased polarity as well as acidity of solvents quenches the fluorescence of both amino acids. Noticeably, the % decrease in the fluorescence intensity of Trp in fluorinated ETHs with respect to ETH is more prominent compared to 7F-Trp. 4F-Trp has been reported to be non-fluorescent in aqueous medium at room temperature [50] but 5F-Trp and 6F-Trp shows comparable fluorescence with that of Trp [51]. The quantum yield of Trp and 7F-Trp in different alcoholic solvents (Table 1) follow the similar trend to the emission as the quantum yield of Trp is significantly higher than 7F-Trp as well as decrease in the quantum yield for the fluorinated alcoholic solvents is higher for Trp than 7F-Trp. The quantum yield of 5F-Trp and 6F-Trp are found to be 0.15 in water [51] which is comparable to Trp (0.14) [52] whereas the quantum yield of 7F-Trp is drastically reduced. Hence, position of substitution in the benzene ring of Trp is very sensitive to its photophysical properties. The fluorescence maxima of Trp do not show any significant peak shift of the emission maxima on the fluorination of ETH solvents whereas a significant blue shift of emission maxima in the case of 7F-Trp is observed in the same set of solvents. The magnitude of the change in the emission maxima and fluorescence intensity of 7F-Trp in alcoholic solvents suggests that the interaction of fluorinated alcoholic solvents may be different from Trp.

Excited state lifetime measurements are essential in order to get the insight of fluorescence properties of a probe molecule in different solvents as steady state spectroscopy provides the average information. Fig. 4 shows the lifetime (τ) traces of Trp and 7F-Trp in ETH, TFE and HFIP, respectively whereas the amplitude and the value of the different components of τ of both probes in alcoholic solvents are depicted in Table 1. It can be seen that two τ components are required to fit the lifetime traces of amino acids in alcoholic solvents. Trp in ETH shows τ components of 1.80 and 4.90 ns with the amplitude of 76% and 24% whereas 7F-Trp in ETH depicts the τ components of 0.80 and 4.50 ns with the amplitude of 61% and 39%, respectively. In earlier study, τ of Trp in ETH has been best fit with three components, although, the excitation wavelength is 296 nm which is different from this study [53]. The value of τ components of Trp decreases in fluorinated-ETHs compared to ETH whereas slight increase in the value of the τ components of 7F-Trp in fluorinated-ETHs was observed than ETH. The different trend of τ components of 7F-Trp in fluorinated-ETHs than Trp suggests that the environment of 7F-Trp in fluorinated-ETHs is different compared to Trp.

The τ of a probe in any solvent medium depends on the dipole moment of probe, polarity of the medium and solute-solvent interaction. Noticeably, $<\tau>$ value of 7F-Trp in ETH (1.16 ns) is significantly less than Trp in same solvent (2.10 ns) which could be due to the higher excited state dipole moment of 7F-Trp (14.75 D) than Trp (10.27 D) in ETH as obtained from the quantum chemical calculation discussed below. The $<\tau>$ value of Trp in fluorinated-ETHs decreases with successive fluorination of solvents. Both the polarity and acidity of fluorinated-ETHs is higher as compared to ETH [54] which causes to decrease the $<\tau>$ of Trp in fluorinated-ETHs. In contrast, $<\tau>$ value of 7F-Trp in different alcoholic solvents increases with the fluorination of ETH which is opposite to the case of Trp. The increase in the $<\tau>$ of 7F-Trp in fluorinated solvents suggests that the polarity of the solvents is not an important factor here and probably the solute-solvent interaction plays a significant role in the fluorescence behavior of 7F-Trp. Interestingly, quantum yield of the 7F-Trp decreases with the fluorination of ETH similar to Trp, however, the $<\tau>$ of 7F-Trp shows the reverse trend in fluorinated

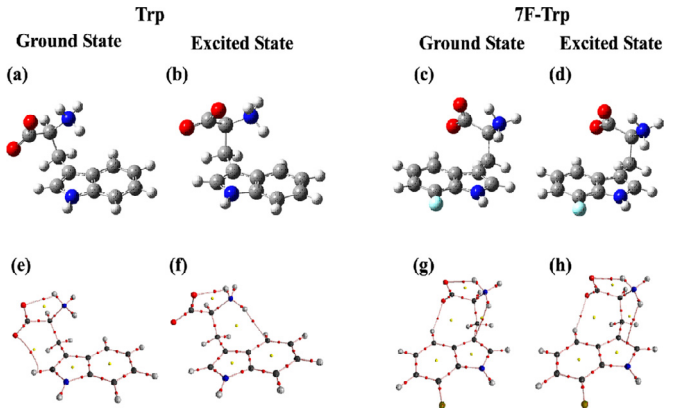

Fig. 5. The most stable structure of Trp (a, b) and 7F-Trp (c, d) in their ground as well as excited states. The molecular graph of the interaction between the different groups of Trp (e, f) and 7F-Trp (g, h) in their ground as well as excited states obtained from the AIM analysis. The bond critical point (BCP) is represented in red point whereas the ring critical point (RCP) is denoted in the yellow color.

ETH as compared to Trp. Further, we have calculated the radiative rate constant (K_r) and non-radiative rate constant (K_{nr}) of Trp and 7F-Trp in alcoholic solvents using Eqs. 1 and 2 to enhance our understanding about their photophysical properties. From the data, it is apparent that the K_r of Trp decreases with the fluorination of ETH and simultaneously K_{nr} increases. In contrast, the K_r of 7F-Trp decreases with the fluorination of ETH, however, the K_{nr} also decreases which is the cause of the absence of correlation between the $<\tau>$ and quantum yield of 7F-Trp in alcoholic solvents.

$$\Phi = \frac{K_r}{K_r + K_{nr}} \quad (1)$$

$$\tau = \frac{1}{K_r + K_{nr}} \quad (2)$$

To decode the molecular basis of the fluorescence properties of amino acids in different alcoholic solvents, we have optimized the monomer of Trp and 7F-Trp with ETH and TFE in the ground as well as excited states. The frequency of each structure shows positive value confirming the minimum energy structure. Further, the peak maxima of the emission of monomer in their respective bulk medium have been calculated to compare with the experimental values. Fig. 5 (a–d) depicts the most stable structure of ground as well as excited states of Trp and 7F-Trp in bulk ETH solvent. The most stable structure of Trp and 7F-Trp do not vary significantly from ground to excited state. However, the orientation of the backbone (NH_3^+ and COO^- groups) of Trp and 7F-Trp is different as the NH_3^+ group of Trp is pointing towards its benzene ring whereas, in the case of 7F-Trp, the orientation of NH_3^+ group is opposite. The most stable structure of Trp and 7F-Trp shows that fluorination of Trp changes its conformation which is in well correlation with the earlier simulation study suggesting that the fluorination of amino acids affects its conformation [55]. The calculated emission maxima of the most stable structure of Trp and 7F-Trp in ETH appears at 313 nm and 289 nm (Table 3), respectively which shows that emission maxima gets blue shifted on the fluorination of Trp which is in the line with the experimental data. It is important to mention that absolute value of the calculated emission maxima of Trp and 7F-Trp is underestimated by ~20–30 nm from its experimental value, however, the trend of the change of emission spectra predicted from the calculation is in agreement with the experimental data. We have also performed the optimization of Trp and 7F-Trp in TFE solvent and the optimized structure of both the amino acids in the ground and excited state is similar to the case of ETH.

Table 2
The energy difference between HOMO and LUMO of Trp and 7F-Trp in both of their ground and excited states in ETH and TFE solvents.

Probe	Solvent	$\Delta E_{HOMO-LUMO}$ (Kcal/mole)	
		Ground state	Excited state
Trp	ETH	165.587	144.704
	TFE	165.593	144.722
7F-Trp	ETH	169.384	150.439
	TFE	169.390	150.477

Table 3
The emission maxima (nm) of Trp and 7F-Trp monomer along with their 1:1 clusters with ETH and TFE have been calculated using the M06-2X/6-31+g(d) level of theory. Polarizable continuum model (PCM) has been used to incorporate the effect of respective solvents.

System	Solvent	Interaction	Emission (nm) (Calculated)	Emission (nm) (experimental)
Monomer				
Trp	ETH		313	335
	TFE		313	335
7F-Trp	ETH		289	320
	TFE		289	310
1:1 cluster				
Trp	ETH	NH…O	318	335
	ETH	COO…HO	314	
	TFE	NH…O	318	335
	TFE	COO…HO	318	
	TFE	NH…F	317	
	TFE	NH_3…O	308	
7F-Trp	ETH	NH…O	289	320
	ETH	COO…HO	289	
	ETH	NH_3…O	287	
	TFE	NH…O	289	310
	TFE	COO…HO	289	
	TFE	NH…F	288	
	TFE	NH_3…O	288	
	TFE	F…F	288	

To explore the nature of electronic transition, highest occupied molecular orbital (HOMO) and lowest unoccupied molecular orbital (LUMO) calculation has been performed (Figure S7 and Table 2). Quantum chemical calculation reveals that combination of several transitions (like HOMO-1, HOMO, LUMO, LUMO-1, LUMO-2 etc.) is responsible for the absorption and emission maxima for both the probes. We have calculated the HOMO→LUMO transition energy to qualitatively compare the trend of experimental data. The HOMO–LUMO energy gap of 7F-Trp is greater than that of Trp in ground and excited states. It confirms that fluorination of Trp destabilizes the excited state causes to show blue shift in both the absorption and emission spectra. Even in all the cases the HOMO–LUMO energy gap is slightly greater in TFE solvent than that of ETH for both the probes indicating the hypsochromic spectral shift with the increase of solvent polarity and acidity which correlates our experimental finding as well. Moreover, from the orbital diagram (Figure S7) it is depicted that for both the probes there are electronic transitions (HOMO→LUMO) from the NH_3^+ containing backbone chain (HOMO) to the indole moiety (LUMO) of the amino acids occurred.

In order to understand the bonding nature of the backbone with the indole ring of the amino acids, we have performed the AIM analysis of the most stable structure of Trp and 7F-Trp in their ground and excited states as shown in Fig. 5(e–h). The presence of (3,-1) bond critical point (BCP) with the electron density (ρ) and Laplacian (L) within the range of 0.002–0.034 a.u. and 0.024–0.139 a.u., respectively [56] represents the non-covalent interaction whereas the (3,+1) ring critical point (RCP) depicts the presence of cyclic structure. Table 4 represents the value of ρ and L for the different BCP between the backbone of amino acids with the indole ring of Trp and 7F-Trp in its ground and excited states. AIM

Table 4
Electron density (ρ) and Laplacian (L) at each bond critical point (BCP) of the interaction between backbone and indole chromophore of both Trp and 7F-Trp at their ground state and excited state obtained from AIM analysis.

System	BCP of interaction	ρ	L(a.u.)
Trp_ground state	$COO^-...H_{(pyrrole)}$	0.00636	0.02408
Trp_excited state	$NH_3^+...C_{(benzene)}$	0.01692	0.05256
7F-Trp_ground state	$COO^-...H_{(benzene)}$	0.01199	0.04176
	$NH_3^+...C_{(pyrrole)}$	0.01526	0.05668
7F-Trp_excited state	$COO^-...H_{(benzene)}$	0.01014	0.03600
	$NH_3^+...C_{(pyrrole)}$	0.01524	0.04792

study of Trp clearly depicts that the local interaction of its backbone with the indole ring is different in the ground and excited states (Fig. 5, e and f). In the ground state of Trp, (3,-1) BCP exists between the backbone COO^- and the C-H group of pyrrole ring along with (3, +1) RCP which indicates the presence of cyclic structure between the backbone and pyrrole ring of Trp through weak C-H….O interaction. In contrast, in the excited state of Trp, the C-H…O interaction disappears and the interaction between the NH_3^+ of the backbone takes place with the benzene ring suggesting the presence of N-H….π interaction. The AIM study suggests that the rotameric state of Trp changes from ground to excited state.

The AIM data of 7F-Trp shows (3,-1) BCP along with (3,+1) RCP for the interactions between COO^- group and C-H of benzene ring as well as NH_3^+ group with pyrrole ring indicating that both NH_3^+ and COO^- groups of the backbone of 7F-Trp interact with its indole group (Fig. 5, g). The excited state structure of 7F-Trp is similar to its ground state (Fig. 5, g and h) except slight variation in the interaction of the backbone with the indole moiety as confirmed by the value of ρ and L shown in Table 4. The AIM study depicts that the interaction of the backbone groups of 7F-Trp with indole moiety is different from Trp in the excited state which is probably one of the reasons behind the decreased fluorescence intensity of 7F-Trp in alcoholic solvents as compared to Trp.

The indole moiety of Trp and 7F-Trp is the main source of the fluorescence; however, its intensity is modulated by the interaction between the backbone of amino acid with the indole ring [57]. It is well known that the ^1L_a state rather than ^1L_b (both states are $\pi\pi*$ in nature) is the main source of the fluorescence emission of indole group of Trp in polar solvents [58]. It has been found that the $\pi\pi*$ states (^1L_a and ^1L_b states) meet at a conical intersection point via a energy barrier which opens nonradiative channel [59]. The tuning of the multiple conical intersections controls the fluorescence intensity as well as lifetime of indole molecules [60]. The fluorescence intensity of indole group in Trp is less than only indole due to the interaction of the backbone side chain of Trp with the indole ring which decreases the barrier between the $\pi\pi*$ states causing to the increased nonradiative rate of fluorescence decay [57]. The AIM data suggests that the interaction of the backbone side chain with the indole ring is enhanced in 7F-Trp than Trp which probably increases the nonradiative rate by lowering the barrier of the conical intersection of $\pi\pi*$ states leading to the decreased fluorescence intensity of 7F-Trp than Trp in alcoholic solvents. Indeed, the recent study on cyno-indole also shows that the presence of electron withdrawing group decreases the fluorescence intensity as compared to indole [61] which is in agreement with our finding about the substitution of electron withdrawing fluorine on Trp. With the increase of the acidity of the solvents, the barrier between the $\pi\pi*$ states of indole group forming the conical intersection is probably decreased; hence, the fluorescence intensity of Trp and 7F-Trp monotonically decreases from ETH to HFIP.

Further, we have optimized different possible structures of 1:1 clusters of Trp and 7F-Trp with ETH and TFE in their respective bulk medium (Fig. 6, S2 and S3). The optimization of each structure has been performed in the ground as well as excited states and the fluorescence maxima of each structure have been computed to correlate it with the experimental values. Two structures of Trp-ETH complexes were found stable, out of which, the N-H group of indole interacts with oxygen of ETH via N-H(ind)….O(ETH) hydrogen bond in the first complex whereas, in the second complex, COO of the backbone of Trp interacts with the OH of ETH through COO(backbone)….HO(ETH) hydrogen bond. The calculated emission maxima of N-H(ind)….O(ETH) hydrogen bonded structure is slightly closer to the experimental value compared to the COO(backbone)….HO(ETH) hydrogen bonded complex. The diversity of the hydrogen bonded structures of Trp with TFE increases than ETH as N-H(indole)…F(TFE) and NH_3(backbone)…OH(TFE) hydrogen bonded structure were found to be stable along with N-H (ind)….O(TFE) and COO(backbone)….HO(TFE) interacted structures. The calculated emission maxima of N-H(ind)….O(TFE), COO(backbone)….HO(TFE) and N-H(indole)…F(TFE) hydrogen bonded complexes are close to the experimental value whereas the emission maxima of NH_3(backbone)…OH(TFE) interacting complex is significantly less than the experimental value suggesting that the contribution of this structure is less in its emission feature.

The N-H(ind)….O(ETH), COO(backbone)….HO(ETH), NH_3(backbone)…OH(ETH) interacting structures were found to be stable for 7F-Trp-ETH complex. The calculated peak maxima of all the structures are almost same and blue shifted compared to Trp-ETH case. It is noticeable that both NH_3^+ and COO^- groups of the backbone chain of 7F-Trp are interacting with ETH which is contrast to Trp case where only COO^- is interacting with ETH. It is apparent from the calculation that the fluorination of Trp enhances the interaction of the backbone chain of 7F-Trp with the solvent molecules. In the case of TFE complex with 7F-Trp, N-H(ind)….O(TFE), COO(backbone)….HO(TFE), NH_3(backbone)…OH(TFE), N-H(ind)….F(TFE) and F(ind)…..F(TFE) interacting structures were found to be stable and their peak maxima are approximately same and closer to the experimental value suggesting the contribution of all these species in their emission spectra. Unlike to other cases, the interaction of the N-H group of indole of 7F-Trp with TFE is cyclic in nature where the N-H(ind)….O(TFE) and O-H(TFE)….F(ind) interactions take place simultaneously (Fig. 6j). Similarly, the N-H(ind)….F(TFE) interaction takes place along with weak F(ind)….F(TFE) interaction and form cyclic structure (Fig. 6l). The interaction of NH_3^+ of the backbone of 7F-Trp with TFE is also cyclic in nature as both the NH_3(backbone)…O(TFE) and NH_3(backbone)…F(TFE) interactions appear simultaneously (Fig. 6m). It is apparent from the quantum chemical calculation that the presence of weak F(ind)….F(TFE), N-H(ind)….F(TFE), NH_3(backbone)…F(TFE) interactions change the solute-solvent interaction of 7F-Trp with TFE compared to Trp case. This finding is in agreement with the experimental study where it has been found that the solute-solvent interactions between 7F-Trp with fluorinated alcohols are different causing different excited state lifetime of 7F-Trp with fluorinated alcohols than Trp.

The MD simulation of Trp and 7F-Trp in ETH and TFE solvents incorporating their excited state charge distribution have been also performed to understand the solvent organization around the amino acids in their excited state. Radial distribution function g(r) between the solvent and the chromophoric indole part as well as the backbone (NH_3^+ and COO^-) of probe molecules have been calculated as shown in Figs. 7 and 8 to get the idea about the solvent orientation around the different sites of probe molecule. The g(r) for the hydrogen bonding of indole N-H group of amino acid with the oxygen of alcoholic solvents decreases for TFE than ETH for Trp and 7F-Trp, both. However, the peak height of the first peak of the g(r) for the N–H(ind)…O(solvent) hydrogen bond of indole group of 7F-Trp in ETH and TFE is less than Trp which indicates that the hydrogen bonding capability of indole group of 7F-Trp is less than Trp (Fig. 7 a and b). However, the possibility of O–H(solvent)…N(ind) is almost same for Trp and 7F-Trp (Fig. 7 c and d). In order to understand the difference in the N–H(ind)…O(solvent) hydrogen bond of indole group of 7F-Trp and Trp with alcoholic solvents, we have probed the interaction of fluorine of 7F-Trp with ETH and TFE by the calculation of g(r) for these interactions as shown in Fig. 7e . The g(r) data

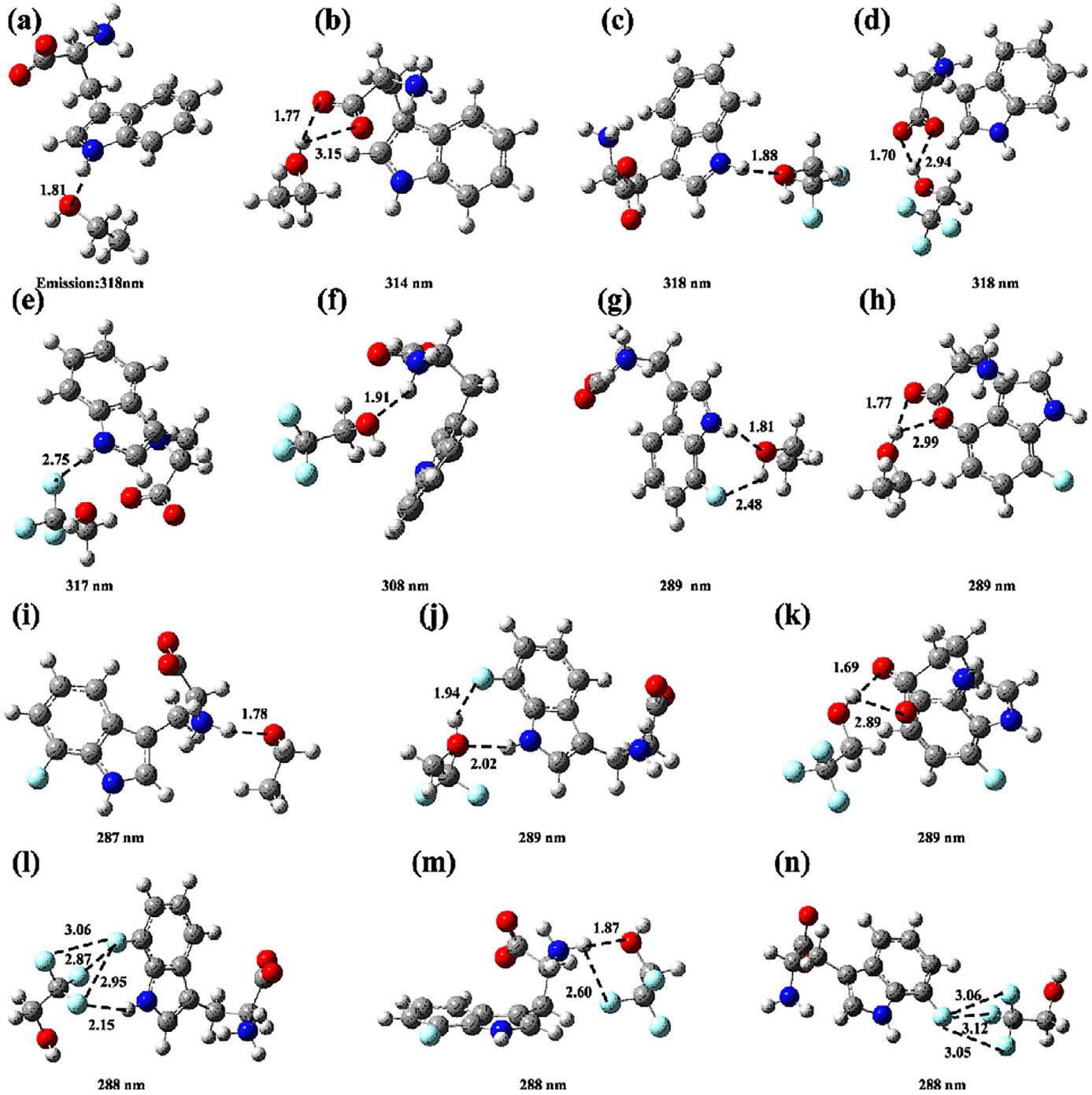

Fig. 6. The excited state optimized 1:1 clusters of Trp (a-f) and 7F-Trp (g-n) with TFE molecule. The corresponding atomic distances and emission maxima obtained from the calculations are mentioned for each structure.

depict the possibility of the extremely weak O-H(alc.)…F(indole) interaction for both ETH and TFE. However, the population of the extremely weak O–H(alc.)…F(7F-Trp) interacted species is slightly higher for the case of TFE than ETH. Apart from that, we have also found the evidence of F(TFE)….F(indole) interaction between the fluorine of TFE and 7F-Trp which probably increases the population of O–H(TFE)…F(7F-Trp) interacted species in TFE. The g(r) data of the fluorine terminal of 7F-Trp with alcoholic solvents suggest that the presence of fluorine changes the interaction of chromophoric indole group of 7F-Trp with alcoholic solvents significantly as compared to Trp which is in agreement with the results obtained from quantum chemical calculation.

Further, we have investigated the effect of fluorination of Trp on the interaction of backbone (NH_3^+ and COO^-) of amino acids with solvent molecules by the calculation of g(r) for different possible interactions as shown in Fig. 8. It is apparent from the g(r) data that the interaction of $COO^-$of Trp and 7F-Trp increases with TFE than ETH (Fig. 8a and 8b). However, the trend is opposite for NH_3^+ as the interaction of NH_3^+ of Trp and 7F-Trp decreases for TFE than ETH. Noticeably, the increase of COO^-…..HO and decrease in NH_3^+…..O interactions of 7F-Trp with TFE is higher than Trp suggesting that the substitution of fluorine modifies the interaction of TFE with the backbone of 7F-Trp. The pattern of the interaction of solvents with the different motifs of Trp and 7F-Trp

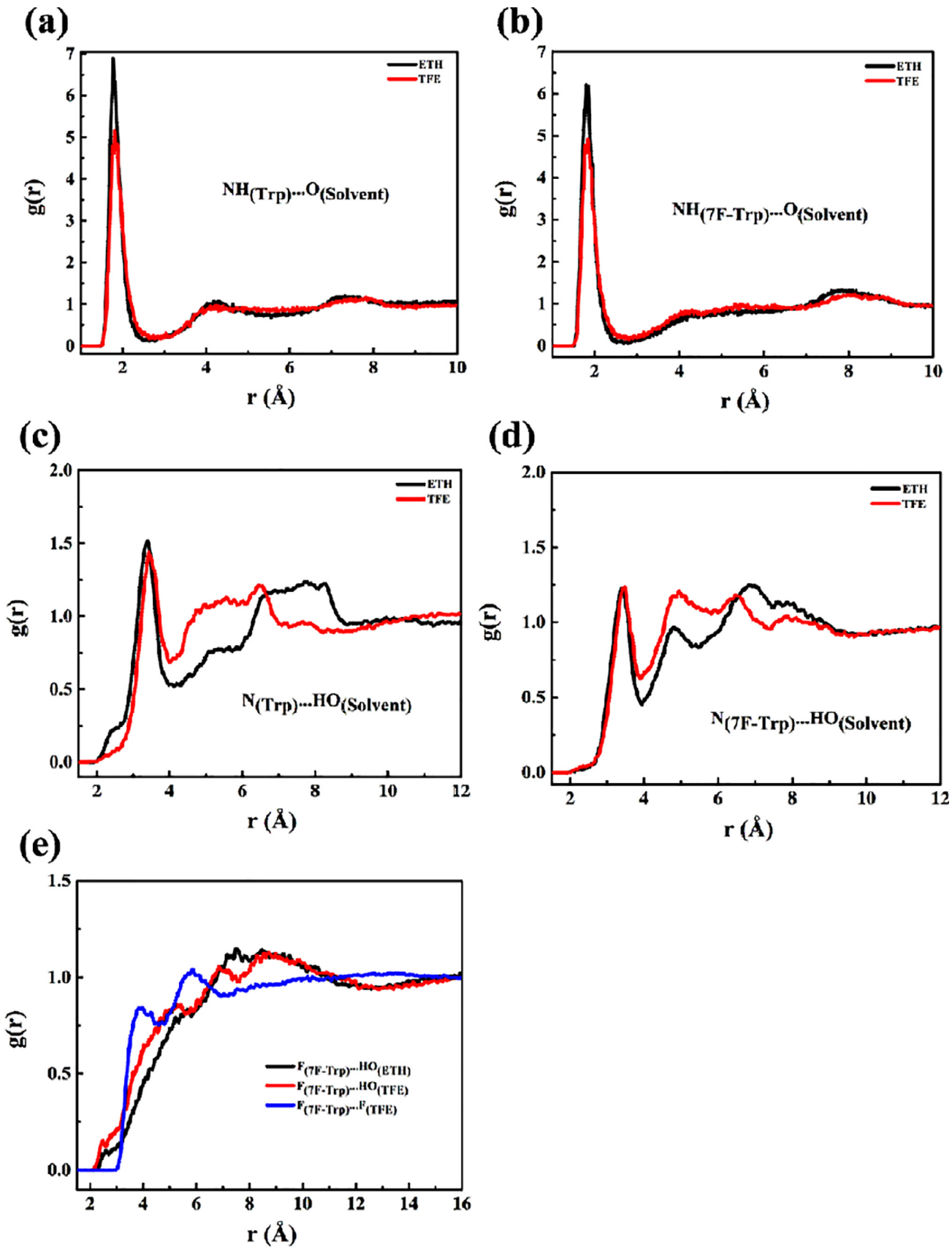

Fig. 7. (a) and (b) represents the g(r) between indole NH (probe) and O (ETH/TFE) of Trp and 7F-Trp, respectively. (c) and (d) represent the g(r) between indole N (probe) and HO (ETH/TFE) of Trp and 7F-Trp, respectively. The g(r) of the interaction of the fluorine terminal of the indole group of 7F-Trp with ETH and TFE solvents is shown in (e) respectively.

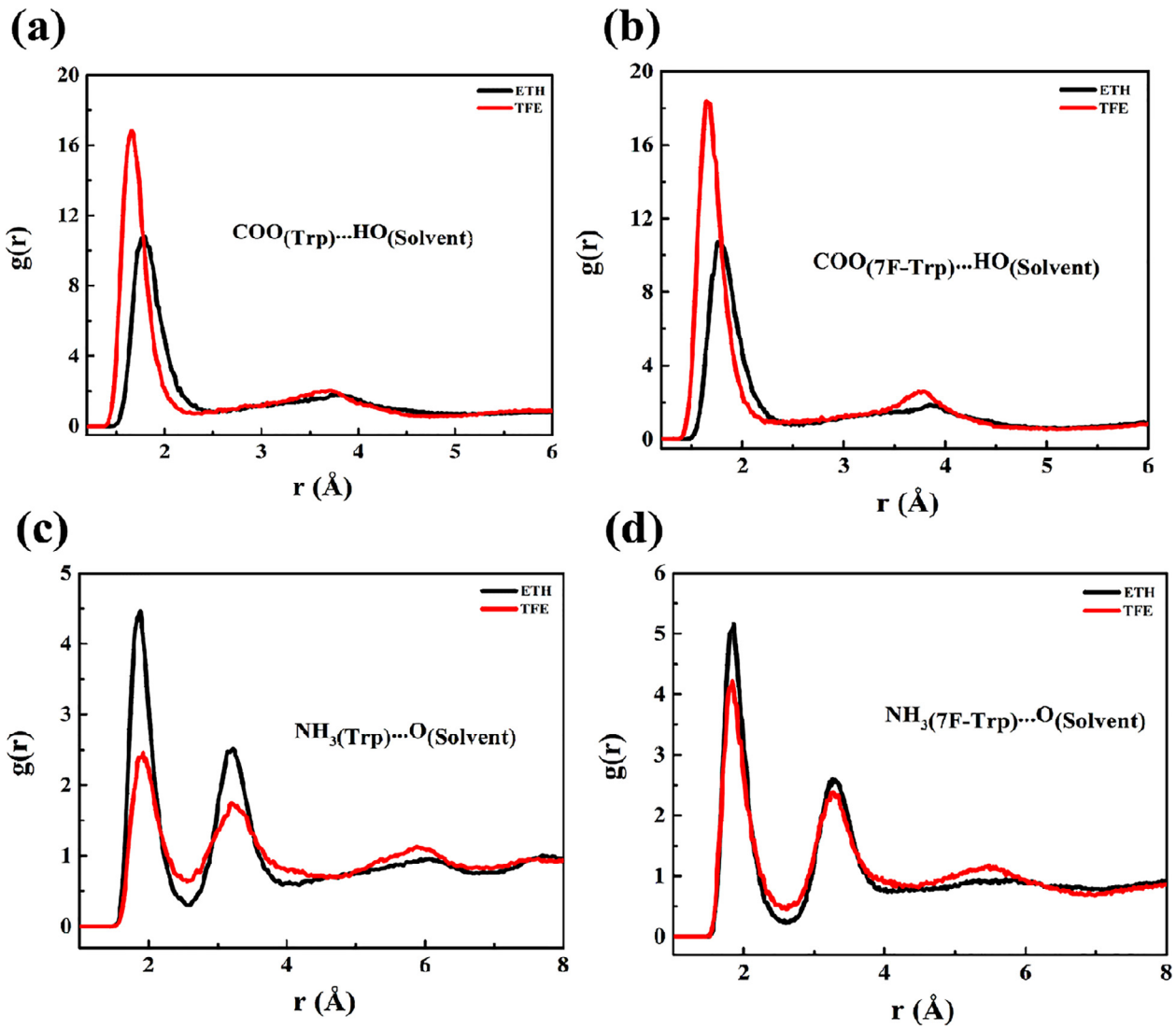

Fig. 8. g(r) for the interaction of the backbone (NH_3^+ and COO^-) of Trp and 7F-Trp with ETH and TFE solvent molecules.

with solvents were also probed in the ground state and the trend of the data is qualitatively similar to the excited state (Figs. S4 and S5).The simulation data suggest that the substitution of fluorine modifies the interaction of indole group as well as backbone of 7F-Trp with alcoholic solvents and the extent of modification for ETH and TFE is different as fluorine of 7F-Trp interacts with fluorine via only O-H(ETH)….F(7F-Trp) whereas TFE can interact through both, O-H(TFE)….F(7F-Trp) and F(TFE)….F(7F-Trp) interactions, apart from other conventional hydrogen bonds which is in line with the observation obtained from the quantum chemical calculation. The experimental, MD simulation and quantum chemical calculation clearly depict that the interaction of fluorine with solvent molecules plays an important role in modulating the photophysical behavior of 7F-Trp in biochemically important alcoholic solvents.

Conclusion

Various spectroscopic methods like UV–visible, fluorescence spectroscopy, excited state lifetime have been utilized to explore the photophysical properties of noncanonical amino acid 7F-Trp in three biochemically important alcoholic solvents ETH, TFE and HFIP. The results obtained have been further compared to its canonical analogue Trp in the same solvents to understand the role of fluorine in the modulation of its photophysical properties. It is found that both the absorption and emission spectra of 7F-Trp are markedly different compared to Trp showing significant blue shift. The trend of excited state lifetime of 7F-Trp is also opposite in those three solvents than that of Trp. To rationalize all these modulation found in the photophysical properties of 7F-Trp we have performed several theoretical calculations like Atoms in molecule (AIM) study, quantum chemical calculation, MD simulation. Surprisingly, quantum chemical calculation shows that the most stable isomer of 7F-Trp is completely different compared to Trp. AIM study of those most stable isomers shows that the substitution of fluorine on tryptophan perturbs the interaction of its backbone containing COO^- and NH_3^+ with the chromophoric indole group which probably decreases the barrier of the conical intersection leading to the decreased fluorescence intensity of 7F-Trp. Although the fluorescence intensity of Trp and 7F-Trp decreases in the presence of fluorinated solvents, the decrease is less in 7F-Trp than Trp. MD simulation also suggests that the excited state lifetime of Trp is controlled by the polarity as well as acidity of the solvent whereas, the solute-solvent interaction plays an important role in the case of 7F-Trp. Fluorine of 7F-Trp interacts weakly with the fluorine and OH terminal of fluorinated alcohols along with conventional hydrogen bonds which control the excited state lifetime of 7F-Trp in fluorinated solvents.

Declaration of Competing Interest

The authors declare that they have no conflict of interest.

Acknowledgments

T.N. acknowledges CSIR for her fellowship. The authors are grateful for the CSS cluster facility and CRAY supercomputing facility of IACS.

Supplementary materials

Supplementary material associated with this article can be found, in the online version, at doi:10.1016/j.jpap.2020.100011.

References

[1] M. Hospes, J. Hendriks, K.J. Hellingwerf, Tryptophan fluorescence as a reporter for structural changes in photoactive yellow protein elicited by photo-activation, Photochem. Photobiol. Sci. 12 (2013) 479–488.
[2] C.A. Royer, Probing protein folding and conformational transitions with fluorescence, Chem. Rev. 106 (2006) 1769–1784.
[3] L. Mátyus, J. Szöllősi, A. Jenei, Steady-state fluorescence quenching applications for studying protein structure and dynamics, J. Photochem. Photobiol., B 83 (2006) 223–236.
[4] L.A. Munishkina, A.L. Fink, Fluorescence as a method to reveal structures and membrane-interactions of amyloidogenic proteins, Biochim. Biophys. Acta, Biomembr. 1768 (2007) 1862–1885.
[5] A. Vallée-Bélisle, S.W. Michnick, Visualizing transient protein-folding intermediates by tryptophan-scanning mutagenesis, Nat. Struct. Mol. Biol. 19 (2012) 731–736.
[6] M.B. Prigozhin, S.-H. Chao, S. Sukenik, T.V. Pogorelov, M. Gruebele, Mapping fast protein folding with multiple-site fluorescent probes, Proc. Natl. Acad. Sci. U.S.A. 112 (2015) 7966.
[7] J.M. Antos, M.B. Francis, Selective tryptophan modification with rhodium carbenoids in aqueous solution, J. Am. Chem. Soc. 126 (2004) 10256–10257.
[8] B.V. Popp, Z.T. Ball, Structure-selective modification of aromatic side chains with dirhodium metallopeptide catalysts, J. Am. Chem. Soc. 132 (2010) 6660–6662.
[9] M. Arias, K.V. Jensen, L.T. Nguyen, D.G. Storey, H.J. Vogel, Hydroxy-tryptophan containing derivatives of tritrpticin: modification of antimicrobial activity and membrane interactions, Biochim. Biophys. Acta, Biomembr. 1848 (2015) 277–288.
[10] N. Budisa, W. Wenger, B. Wiltschi, Residue-specific global fluorination of Candida antarctica lipase B in Pichia pastoris, Mol Biosyst. 6 (2010) 1630–1639.
[11] T. He, A. Gershenson, S.J. Eyles, Y.-J. Lee, W.R. Liu, J. Wang, J. Gao, M.F. Roberts, Fluorinated aromatic amino acids distinguish cation-π interactions from membrane insertion, J. Biol. Chem. 290 (2015) 19334–19342.
[12] N.K. Mishra, A.K. Urick, S.W.J. Ember, E. Schönbrunn, W.C. Pomerantz, Fluorinated aromatic amino acids are sensitive 19F NMR probes for bromodomain-ligand interactions, ACS Chem. Biol. 9 (2014) 2755–2760.
[13] N.C. Yoder, K. Kumar, Fluorinated amino acids in protein design and engineering, Chem. Soc. Rev. 31 (2002) 335–341.
[14] B. Bilgiçer, X. Xing, K. Kumar, Programmed self-sorting of coiled coils with leucine and hexafluoroleucine cores, J. Am. Chem. Soc. 123 (2001) 11815–11816.
[15] B. Bilgiçer, K. Kumar, Synthesis and thermodynamic characterization of self-sorting coiled coils, Tetrahedron 58 (2002) 4105–4112.
[16] E.A. Pratt, C. Ho, Incorporation of fluorotryptophans into proteins of Escherichia coli, Biochemistry 14 (1975) 3035–3040.
[17] J.C. Biffinger, H.W. Kim, S.G. DiMagno, The polar hydrophobicity of fluorinated compounds, Chem. BioChem 5 (2004) 622–627.
[18] O.-H. Kwon, T.H. Yoo, C.M. Othon, J.A. Van Deventer, D.A. Tirrell, A.H. Zewail, Hydration dynamics at fluorinated protein surfaces, Proc. Natl. Acad. Sci. U.S.A. 107 (2010) 17101.
[19] J. Xu, B. Chen, P. Callis, P.L. Muiño, H. Rozeboom, J. Broos, D. Toptygin, L. Brand, J.R. Knutson, Picosecond fluorescence dynamics of tryptophan and 5-fluorotryptophan in monellin: slow water–protein relaxation unmasked, J. Phys. Chem. B 119 (2015) 4230–4239.
[20] S.S. Sarkar, J.B. Udgaonkar, G. Krishnamoorthy, Reduced fluorescence lifetime heterogeneity of 5-fluorotryptophan in comparison to tryptophan in proteins: implication for resonance energy transfer experiments, J. Phys. Chem. B 115 (2011) 7479–7486.
[21] B.D. Zlatopolskiy, J. Zischler, D. Schäfer, E.A. Urusova, M. Guliyev, O. Bannykh, H. Endepols, B. Neumaier, Discovery of 7- [18F]Fluorotryptophan as a novel positron emission tomography (PET) probe for the visualization of tryptophan metabolism in vivo, J. Med. Chem. 61 (2018) 189–206.
[22] N.W.S. Davies, G. Guillemin, B.J. Brew, Tryptophan, neurodegeneration and HIV-associated neurocognitive disorder, Int. J. Tryptophan Res. 3 (2010) 121–140.
[23] G.F. Oxenkrug, Tryptophan metabolism as a new target for the treatment of schizophrenia, US Psychiatry Rev. (2007) 38–39.
[24] J.F. Povey, C.M. Smales, S.J. Hassard, M.J. Howard, Comparison of the effects of 2,2,2-trifluoroethanol on peptide and protein structure and function, J. Struct. Biol. 157 (2007) 329–338.
[25] D. Roccatano, G. Colombo, M. Fioroni, A.E. Mark, Mechanism by which 2,2,2-trifluoroethanol/water mixtures stabilize secondary-structure formation in peptides: a molecular dynamics study, Proc. Natl. Acad. Sci. U.S.A. 99 (2002) 12179.
[26] R.L. Taber, The competitive inhibition of yeast alcohol dehydrogenase by 2,2,2-trifluoroethanol, Biochem. Educ. 26 (1998) 239–242.
[27] I.K. Herrmann, M. Castellon, D.E. Schwartz, M. Hasler, M. Urner, G. Hu, R.D. Minshall, B. Beck-Schimmer, Intravenous application of a primary sevoflurane metabolite improves outcome in murine septic peritonitis: first results, PLOS One 8 (2013) e72057.
[28] J.T. Gerig, Structure and solvation of melittin in 1,1,1,3,3,3-hexafluoro-2-propanol/water, Biophys. J. 86 (2004) 3166–3175.
[29] M. Urner, M. Schläpfer, I.K. Herrmann, M. Hasler, R.R. Schimmer, C. Booy, B. Roth Z'graggen, H. Rehrauer, F. Aigner, R.D. Minshall, W.J. Stark, B. Beck-Schimmer, Insight into the beneficial immunomodulatory mechanism of the sevoflurane metabolite hexafluoro-2-propanol in a rat model of endotoxaemia, Clin. Exp. Immunol. 181 (2015) 468–479.
[30] L. Wang, D. Wang, F. Li, Insight into the structures of the second and fifth transmembrane domains of Slc11a1 in membrane mimics, J. Pept. Sci. 20 (2014) 165–172.
[31] V. Booth, A.J. Waring, F.J. Walther, K.M.W. Keough, NMR structures of the C-terminal segment of surfactant protein B in detergent micelles and hexafluoro-2-propanol, Biochemistry 43 (2004) 15187–15194.
[32] Y. Zhao, D.G. Truhlar, The M06 suite of density functionals for main group thermochemistry, thermochemical kinetics, noncovalent interactions, excited states, and transition elements: two new functionals and systematic testing of four M06-class functionals and 12 other functionals, Theor. Chem. Acc. 120 (2008) 215–241.
[33] S. Miertuš, E. Scrocco, J. Tomasi, Electrostatic interaction of a solute with a continuum. A direct utilizaion of AB initio molecular potentials for the prevision of solvent effects, Chem. Phys. 55 (1981) 117–129.
[34] B. Mennucci, J. Tomasi, R. Cammi, J.R. Cheeseman, M.J. Frisch, F.J. Devlin, S. Gabriel, P.J. Stephens, Polarizable continuum model (PCM) calculations of solvent effects on optical rotations of chiral molecules, J. Phys. Chem. A 106 (2002) 6102–6113.
[35] M.J. Frisch, G.W. Trucks, H.B. Schlegel, G.E. Scuseria, M.A. Robb, J.R. Cheeseman, G. Scalmani, V. Barone, G.A. Petersson, H. Nakatsuji, X. Li, M. Caricato, A.V. Marenich, J. Bloino, B.G. Janesko, R. Gomperts, B. Mennucci, H.P. Hratchian, J.V. Ortiz, A.F. Izmaylov, J.L. Sonnenberg, Williams, F. Ding, F. Lipparini, F. Egidi, J. Goings, B. Peng, A. Petrone, T. Henderson, D. Ranasinghe, V.G. Zakrzewski, J. Gao, N. Rega, G. Zheng, W. Liang, M. Hada, M. Ehara, K. Toyota, R. Fukuda, J. Hasegawa, M. Ishida, T. Nakajima, Y. Honda, O. Kitao, H. Nakai, T. Vreven, K. Throssell, J.A. Montgomery Jr., J.E. Peralta, F. Ogliaro, M.J. Bearpark, J.J. Heyd, E.N. Brothers, K.N. Kudin, V.N. Staroverov, T.A. Keith, R. Kobayashi, J. Normand, K. Raghavachari, A.P. Rendell, J.C. Burant, S.S. Iyengar, J. Tomasi, M. Cossi, J.M. Millam, M. Klene, C. Adamo, R. Cammi, J.W. Ochterski, R.L. Martin, K. Morokuma, O. Farkas, J.B. Foresman, D.J. Fox, Gaussian 16 Rev. A.03, in, Gaussian 16, Rev. A.03, Wallingford, CT, 2016.
[36] AIM2000, J. Comput. Chem. 22 (2001) 545–559.
[37] D.v.d.S.M.J. Abraham, E. Lindahl and B. Hess and the GROMACS development team, (2016).
[38] W.L. Jorgensen, J. Tirado-Rives, The OPLS [optimized potentials for liquid simulations] potential functions for proteins, energy minimizations for crystals of cyclic peptides and crambin, J. Am. Chem. Soc. 110 (1988) 1657–1666.
[39] W.L. Jorgensen, J. Tirado-Rives, Potential energy functions for atomic-level simulations of water and organic and biomolecular systems, Proc. Nat. Acad. Sci. USA 102 (2005) 6665.
[40] L.S. Dodda, I. Cabeza de Vaca, J. Tirado-Rives, W.L. Jorgensen, LigParGen web server: an automatic OPLS-AA parameter generator for organic ligands, Nucl. Acids Res 45 (2017) W331–W336.
[41] L.S. Dodda, J.Z. Vilseck, J. Tirado-Rives, W.L. Jorgensen, 1.14*CM1A-LBCC: localized bond-charge corrected CM1A charges for condensed-phase simulations, J. Phys. Chem. B 121 (2017) 3864–3870.
[42] M. Parrinello, A. Rahman, Polymorphic transitions in single crystals: a new molecular dynamics method, J. Appl. Phys. 52 (1981) 7182–7190.
[43] H.J.C. Berendsen, J.P.M. Postma, W.F.v. Gunsteren, A. DiNola, J.R. Haak, Molecular dynamics with coupling to an external bath, J. Chem. Phys. 81 (1984) 3684–3690.
[44] D.S. Frenkel, S. Berend, Understanding molecular simulation: from algorithms to applications, Comput. Sci. Ser. 1 (2002) 1–638.
[45] J.Y.C. Lim, P.D. Beer, Sigma-hole interactions in anion recognition, Chemistry 4 (2018) 731–783.
[46] T. Clark, M. Hennemann, J.S. Murray, P. Politzer, Halogen bonding: the sigma–hole. Proceedings of "Modeling interactions in biomolecules II", Prague, September 5th-9th, 2005, J. Mol. Model. 13 (2007) 291–296.
[47] W.L. Jorgensen, P. Schyman, Treatment of halogen bonding in the OPLS-AA force field: application to potent anti-HIV agents, J. Chem. Theory Comput. 8 (2012) 3895–3901.
[48] P. Politzer, J.S. Murray, T. Clark, Halogen bonding and other σ-hole interactions: a perspective, Phys. Chem. Chem. Phys. 15 (2013) 11178–11189.
[49] J.R. Platt, Classification of spectra of cata-condensed hydrocarbons, J. Chem. Phys. 17 (1949) 484–495.
[50] J.L. Hott, R.F. Borkman, The non-fluorescence of 4-fluorotryptophan, Biochem. J. 264 (1989) 297–299.
[51] K. Lotte, R. Plessow, A. Brockhinke, Static and time-resolved fluorescence investigations of tryptophan analogues – a solvent study, Photochem. Photobiol. Sci. 3 (2004) 348–359.
[52] J. Eisinger, G. Navon, Fluorescence quenching and isotope effect of tryptophan, J. Chem. Phys. 50 (1969) 2069–2077.
[53] J.R. Albani, Origin of tryptophan fluorescence lifetimes part 1. Fluorescence lifetimes origin of tryptophan free in solution, J. Fluoresc. 24 (2014) 93–104.
[54] C. Reichardt, Empirical parameters of solvent polarity as linear free-energy relationships, Angew. Chem. Int. Ed. Engl. 18 (1979) 98–110.

[55] J.R. Robalo, A. Vila Verde, Unexpected trends in the hydrophobicity of fluorinated amino acids reflect competing changes in polarity and conformation, Phys. Chem. Chem. Phys. 21 (2019) 2029–2038.
[56] X. Niu, Z. Huang, L. Ma, T. Shen, L. Guo, Density functional theory, natural bond orbital and quantum theory of atoms in molecule analyses on the hydrogen bonding interactions in tryptophan-water complexes, J. Chem. Sci. 125 (2013) 949–958.
[57] L. Blancafort, D. González, M. Olivucci, M.A. Robb, Quenching of tryptophan 1(π,π^*) fluorescence induced by intramolecular hydrogen abstraction via an aborted decarboxylation mechanism, J. Am. Chem. Soc. 124 (2002) 6398–6406.
[58] J. Catalán, x Dı, C. az, First reported evidence that solvent polarity induces an 1Lb↔1La inversion in the indole chromophore, Chem. Phys. Lett. 368 (2003) 717–723.
[59] A. Giussani, M. Merchán, D. Roca-Sanjuán, R. Lindh, Essential on the photophysics and photochemistry of the indole chromophore by using a totally unconstrained theoretical approach, J. Chem. Theory Comput. 7 (2011) 4088–4096.
[60] M. Schneider, M.-L. Hebestreit, M.M. Lindic, H. Parsian, A.Y. Torres-Boy, L. Álvarez–Valtierra, W.L. Meerts, R. Kühnemuth, M. Schmitt, Rotationally resolved electronic spectroscopy of 3-cyanoindole and the 3-cyanoindole–water complex, Phys. Chem. Chem. Phys. 20 (2018) 23441–23452.
[61] M.R. Hilaire, D. Mukherjee, T. Troxler, F. Gai, Solvent dependence of cyanoindole fluorescence lifetime, Chem. Phys. Lett. 685 (2017) 133–138.